Anomalies of Visceroatrial Situs

Subha Ghosh[1,2]
Gail Yarmish[1,3]
Alla Godelman[1]
Linda B. Haramati[1]
Hugo Spindola-Franco[1]

OBJECTIVE. Visceroatrial situs refers to the position and configuration of the cardiac atria, the tracheobronchial tree, and the thoracoabdominal viscera. Accurate determination of situs is essential because anomalies of situs are associated with an increased incidence of complex congenital heart disease.

CONCLUSION. We propose a methodical diagnostic approach to determining the visceroatrial situs and cardiac configuration that predicts the probability and types of associated congenital heart disease.

Visceroatrial situs refers to the position and configuration of the cardiac atria, the tracheobronchial tree, and the abdominal viscera [1]. Abnormalities of visceroatrial situs are often associated with complex congenital heart disease (CHD) [2]. In this article we describe a methodical approach to determining visceroatrial situs and cardiac position to elucidate the spectrum of associated cardiac anomalies. Thus, the probability and type of CHD associated with specific situs anomalies can be accurately predicted [3].

Diagnostic Algorithm

The atria maintain their laterality throughout development; hence, they define the cardiac situs. The thoracic (tracheobronchial) situs is concordant with the cardiac situs in most people. Therefore, the key to diagnosing abnormalities of visceroatrial situs on chest imaging lies in the correct identification of the anatomically distinctive tracheobronchial tree [4, 5]. The morphologic right main bronchus is eparterial and is consistently located above the morphologic right atrium, whereas the left main bronchus is hyparterial and is consistently located above the left atrium (Fig. 1). In patients with situs abnormalities, typical landmarks that differentiate the atria, such as the systemic and pulmonary venoatrial connections, the crista terminalis, and the pectinate muscles, do not conform to the usual anatomy and prove less useful than the tracheobronchial anatomy, which remains distinguishable on chest radiography.

The configuration of the tracheobronchial tree does not predict the position of the ventricles, the great vessels, or the cardiac apex, which must be specifically noted. We diagram a methodical approach to determining the thoracic and cardiac situs and position (Fig. 2) that predicts the probability and types of associated CHD.

Embryology of Cardiac Situs and Atrioventricular Relationships

The embryonic cardiac tube shows pulsatility on day 22 and undergoes constrictions that outline future cardiac chambers (Fig. 3). The position of the atria, as opposed to the primitive ventricle or the bulbus cordis, determines the cardiac situs because only the atria fully retain their laterality throughout cardiac development [6]. Cardiac situs solitus is present when a morphologic right atrium is located to the right of a morphologic left atrium. Situs inversus represents a mirror-image configuration with a morphologic right atrium located to the left of a morphologic left atrium.

The cardiac tube undergoes looping at day 23. With D looping, the bulbus cordis is located to the right of the primitive ventricle. The proximal bulbus cordis gives rise to the right ventricle, and the primitive ventricle forms the morphologic left ventricle. Hence, in situs solitus with D looping, atrioventricular concordance is established as the right atrium connects to the right ventricle and the left atrium to the left ventricle. The cardiac mass (ventricles) then undergoes horizontal shift (version) from right to left, resulting in

Keywords: cardiopulmonary imaging, congenital heart disease, situs, visceroatrial situs

DOI:10.2214/AJR.09.2411

Received January 21, 2009; accepted after revision March 29, 2009.

[1]Department of Radiology, Albert Einstein College of Medicine, Montefiore Medical Center, 111 E 210 St., Bronx, NY 10467. Address correspondence to L. B. Haramati.

[2]Present address: Department of Radiology, Ohio State University Medical Center, Columbus, OH.

[3]Present address: Department of Radiology, Staten Island University Hospital, Staten Island, NY.

CME
This article is available for CME credit.
See www.arrs.org for more information.

AJR 2009; 193:1107–1117

0361–803X/09/1934–1107

the normal orientation of the apex toward the left [1, 6]. Therefore, normal is represented by cardiac situs solitus with D looping, atrioventricular concordance, and levoversion or levocardia (Fig. 4). A partial apical shift results in a midline apex in which mesoversion or mesocardia and failure of apical shift result in dextroversion or dextrocardia (Fig. 5).

With L looping, the bulbus cordis is to the left of the primitive ventricle. Hence, in situs solitus with L looping, there is atrioventricular discordance [7]. The degree of horizontal shift then determines the location of the cardiac apex. Similarly, an L loop in situs inversus results in atrioventricular concordance, whereas a D loop results in atrioventricular discordance. The degree of shift of the cardiac apex then further classifies these forms [1, 6–8].

Thoracic and Abdominal Situs

In humans, most of the thoracic and abdominal viscera are normally asymmetric and lateralized. Situs solitus with levoversion is the normal anatomic state, with a trilobed right lung and a bilobed left lung; the morphologic right atrium is to the right of the morphologic left atrium and the cardiac apex is left-sided. Situs inversus with dextroversion refers to a mirror image of situs solitus. The incidence and severity of complex CHD are proportional to the failure of shift of the cardiac apex with respect to the cardiac situs. There is a greater than 90% incidence of severe CHD in both situs solitus with dextroversion and situs inversus with levoversion [8]. The incidence of CHD in situs solitus and situs inversus with mesoversion is similar to situs solitus with levoversion. For example, situs solitus with dextroversion is often associated with cyanotic defects such as pulmonary atresia or stenosis and tricuspid atresia, whereas situs solitus or situs inversus with mesoversion may have no associated cardiac abnormality or may be linked to CHD, especially levotransposition of the great vessels [1] (Fig. 6).

Commonly, the thoracic and the abdominal viscera are concordant with the normal position described as situs solitus totalis, with an incidence of CHD of 0.8%. Similarly, situs inversus totalis is the mirror image of situs solitus totalis (Fig. 7), with an incidence of CHD of 3–5%. Twenty percent of patients with situs inversus totalis have Kartagener's syndrome [9, 10], a variant of primary ciliary dyskinesia characterized by the triad of situs inversus, chronic sinusitis, and bronchiectasis [11] (Fig. 8). Rarely, the abdominal viscera may be discordant with respect to thoracic situs, resulting in thoracoabdominal discordance, which has a high incidence of associated CHD [1].

Heterotaxy Syndromes

Failure of normal lateralization results in abnormal bilateral symmetry of normally asymmetric viscera and duplication of either right- or left-sided structures. These conditions present with indeterminate situs or situs ambiguous and are often referred to as isomerism or heterotaxy syndromes. Heterotaxy syndromes are usually associated with CHD and splenic abnormalities [12, 13]. The major forms include asplenia or Ivemark's syndrome [14] and polysplenia syndrome.

Asplenia is characterized by an absent spleen and duplication of right-sided structures (bilateral right-sidedness) [1, 2, 15], affecting males twice as commonly as females. Bilateral right-sidedness anomalies include bilateral trilobed lungs with eparterial bronchi (Fig. 9). Cardiac anomalies associated with asplenia are usually severe, are present at an early age, and have a poor prognosis. A single ventricle or large ventricular septal defect and pulmonic stenosis or atresia commonly occurs, resulting in undercirculation and cyanosis. Both systemic and pulmonary venous drainage may be anomalous. Characteristically, the inferior vena cava (IVC) and the abdominal aorta have a common course, with the abdominal aorta being juxtaposed to the IVC, and together they traverse the midline just below the diaphragm to enter a common atrium. Total anomalous pulmonary venous return (Fig. 10) and malposition of the great arteries are frequently associated with asplenia. Bilateral superior venae cavae (SVC) drain into a common atrium with features of bilateral right atria.

Noncardiac findings include an absent spleen and transverse liver, with the stomach on either side. Bowel malrotation, gallbladder agenesis, imperforate anus, horseshoe kidneys, and urethral valves are associated with asplenia [16]. An absent spleen results in life-threatening infections at an early age and Howell-Jolly bodies on peripheral blood smear.

Polysplenia syndrome [1, 2, 17–19] is characterized by duplication of left-sided structures, with bilateral bilobed lungs and hyparterial bronchi and bilateral left atria (Fig. 11). It has a slight female predominance and a milder course than asplenia. One quarter of patients do not have significant cardiac anomalies. CHD commonly associated with polysplenia includes endocardial cushion defects (Fig. 12), double-outlet right ventricle, and left heart obstruction, such as coarctation of the aorta. Abnormalities of systemic venous drainage are common and include interruption of the intrahepatic IVC with azygos continuation, duplication of the SVC, and partial anomalous pulmonary venous return. Abdominal anomalies include multiple small rounded spleens, a symmetric or transverse liver, biliary atresia, and malrotation of the bowel [20, 21].

Minor forms of situs ambiguous include M-anisosplenia or third syndrome and F-anisosplenia or fourth syndrome [1] (Fig. 13). They are characterized by a bifurcated spleen and bronchial symmetry. M-anisosplenia is more common in males and resembles a mild form of asplenia with bilateral eparterial bronchi. Associated cardiac anomalies include anomalous pulmonary venous return, common atrium, pulmonary stenosis, and bilateral SVC. F-anisosplenia is more common in females and resembles a severe form of polysplenia with bilateral hyparterial bronchi. Associated cardiac anomalies include double-outlet right ventricle, bilateral SVC, and azygos continuation of the IVC.

Conclusion

In conclusion, a methodical diagnostic approach using the tracheobronchial tree, the position of the cardiac apex, and the position of the abdominal viscera provides a practical algorithm, applicable to chest radiography, that predicts the risk of CHD and specific associations. In the normal state (situs solitus totalis), the risk of CHD is 0.8%. In situs inversus totalis (Fig. 14) the risk of CHD is 3–5%. If the cardiac version is the opposite of expected, the risk of CHD is 90–100%. In heterotaxy, there is bilateral symmetry of normally asymmetric anatomy. Asplenia has bilateral right-sided (eparterial) bronchial anatomy (Fig. 15) and is associated with CHD in 99–100% of cases. Polysplenia has bilateral left-sided (hyparterial) bronchial anatomy (Fig. 16) and is associated with CHD in 75% of cases.

Acknowledgment

We thank Adina Haramati for her expert schematic illustrations.

References

1. Spindola-Franco H, Fish BG. *Radiology of the heart: cardiac imaging in infants, children and adults*. New York, NY: Springer-Verlag, 1985:

620–637
2. Tonkin IL, Tonkin AK. Visceroatrial situs abnormalities: sonographic and computed tomographic appearance. *AJR* 1982; 138:509–515
3. Hernanz-Schulman M, Ambrosino MM, Genieser NB, et al. Current evaluation of the patient with abnormal visceroatrial situs. *AJR* 1990; 154:797–802
4. Van Mierop LHS, Eisen S, Schiebler GL. The radiographic appearance of the tracheobronchial tree as an indicator of visceral situs. *Am J Cardiol* 1970; 26:432–435
5. Landing BH. Syndromes of congenital heart disease with tracheobronchial anomalies. Edward B. D. Neuhauser Lecture, 1974. *Am J Roentgenol Radium Ther Nucl Med* 1975; 123:679–686
6. Angelini P. Embryology and congenital heart disease. *Tex Heart Inst J* 1995; 22:1–12
7. Shaher RM, Duckworth JW, Khoury GH, Moes CA. The significance of the atrial situs in the diagnosis of positional anomalies of the heart. *Am Heart J* 1967; 73:32–48
8. Van Praagh R, Vlad P. Dextrocardia, mesocardia and levocardia: the segmental approach to diagnosis in congenital heart disease. In: Keith JD, Rowe RD, Vlad P, eds. *Heart disease in infancy and childhood,* 3rd ed. New York, NY: Macmillan, 1978:638–695
9. Kennedy MP, Omran H, Leigh MW, et al. Congenital heart disease and other heterotaxic defects in a large cohort of patients with primary ciliary dyskinesia. *Circulation* 2007; 115:2814–2821
10. Kartagener M, Stucki P. Bronchiectasis with situs inversus. *Arch Pediatr* 1962; 79:193–207
11. Yarnal JR, Golish JA, Ahmad M, Tomashefski JF. The immotile cilia syndrome: explanation for many a clinical mystery. *Postgrad Med* 1982; 71:195–217
12. Applegate KE, Goske MJ, Pierce G, Murphy D. Situs revisited: imaging of the heterotaxy syndrome. *RadioGraphics* 1999; 19:837–852
13. Winer-Muram HT, Tonkin ILD. The spectrum of heterotaxic syndromes. *Radiol Clin North Am* 1989; 27:1147–1170
14. Ivemark BI. Implications of agenesis of the spleen on the pathogenesis of conotruncus anomalies in childhood: analysis of the heart malformations in splenic agenesis syndrome, with fourteen new cases. *Acta Paediatr Suppl* 1955; 44[suppl 104]:7–110
15. Phoon CK, Neill CA. Asplenia syndrome: insight into embryology through an analysis of cardiac and extracardiac anomalies. *Am J Cardiol* 1994; 73:581–587
16. Freedom RM. The asplenia syndrome: a review of significant extracardiac structural abnormalities in 29 necropsied patients. *J Pediatr* 1972; 81: 1130–1133
17. Vossen PG, van Hedent EF, Degryse HR, de Shepper AM. Computed tomography of the polysplenia syndrome in the adult. *Gastrointest Radiol* 1987; 12:209–211
18. Winer-Muram HT, Tonkin ILD, Gold RE. Polysplenia syndrome in the asymptomatic adult: computed tomography evaluation. *J Thorac Imaging* 1991; 6:69–71
19. Peoples WM, Moller JH, Edwards JE. Polysplenia: a review of 146 cases. *Pediatr Cardiol* 1983; 4:129–137
20. Ditchfield MR, Hutson JM. Intestinal rotational abnormalities in polysplenia and asplenia syndromes. *Pediatr Radiol* 1998; 28:303–306
21. Gagner M, Munson L, Scholz FJ. Hepatobiliary anomalies associated with polysplenia syndrome. *Gastrointest Radiol* 1991; 16:167–171

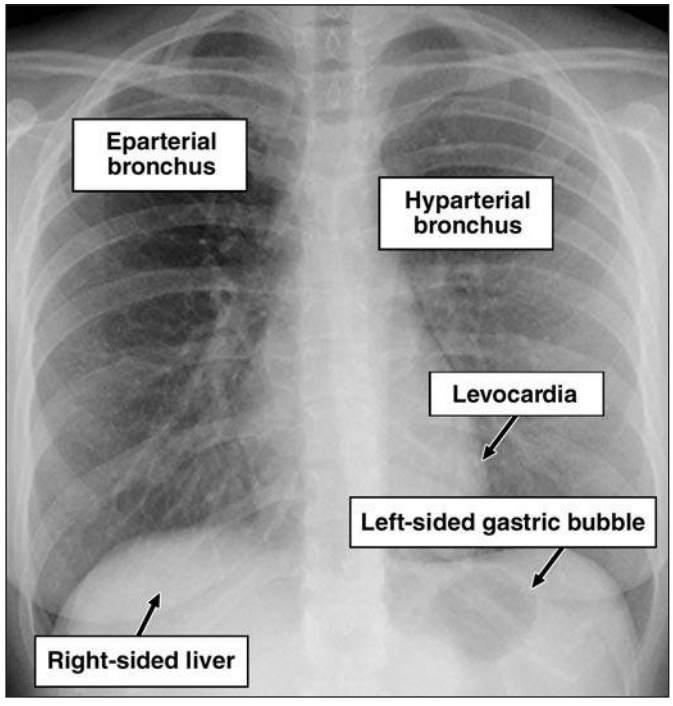

Fig. 1—Posteroanterior chest radiograph in 27-year-old woman with situs solitus totalis. This is normal orientation. Incidence of congenital heart disease is 0.8%.

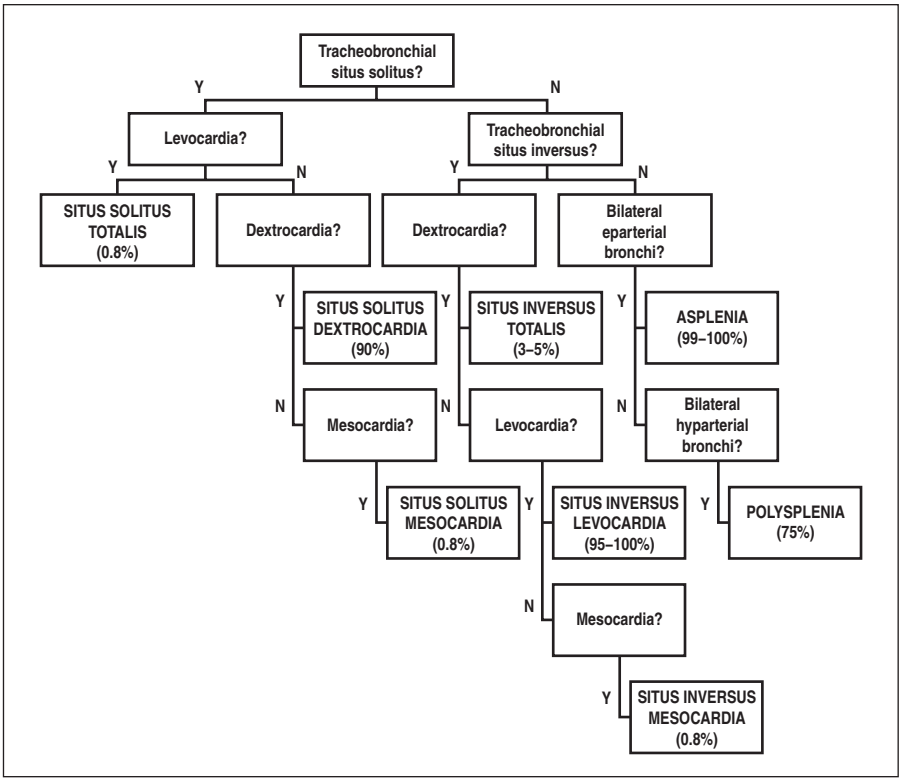

Fig. 2—Diagram of methodical approach to determine visceroatrial situs using configuration of tracheobronchial tree and position of cardiac apex. This is useful in predicting probability (percentage) and types of associated congenital heart disease.

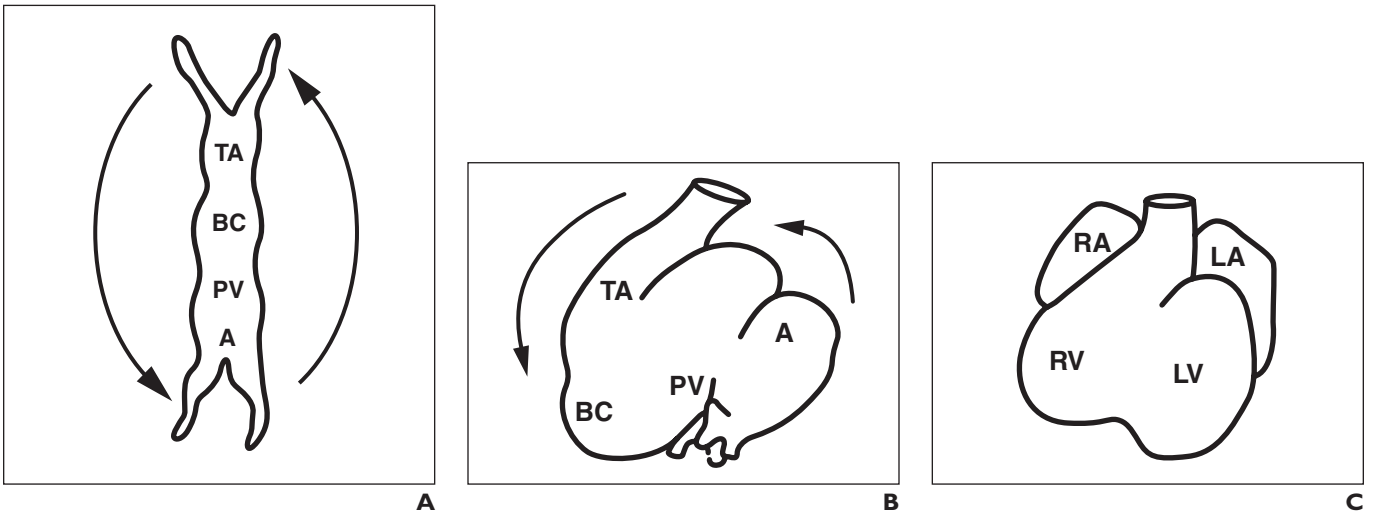

Fig. 3—Diagrams show configuration of primitive heart and sequence of normal D looping.
A and **B,** Primitive cardiac tube undergoes constrictions that outline future cardiac chambers (**A**). Looping of bulboventricular tube results in cephalic end of tube bending caudally and ventrally with respect to paired atria (**B**). Thus, atria are located dorsally and cephalad to primitive ventricle and bulbus cordis. TA = truncus arteriosus, BC = bulbus cordis, PV = primitive ventricle, A = right or left atrium.
C, With D looping, bulbus cordis (precursor of right ventricle) is located to right of primitive ventricle (RV; precursor of left ventricle). Proximal portion of bulbus cordis gives rise to right ventricle (RV), and primitive ventricle forms morphologic left ventricle (LV). Hence, in situs solitus with D looping, atrioventricular concordance is established as right atrium (RA) connects to right ventricle and left atrium (LA) to left ventricle.

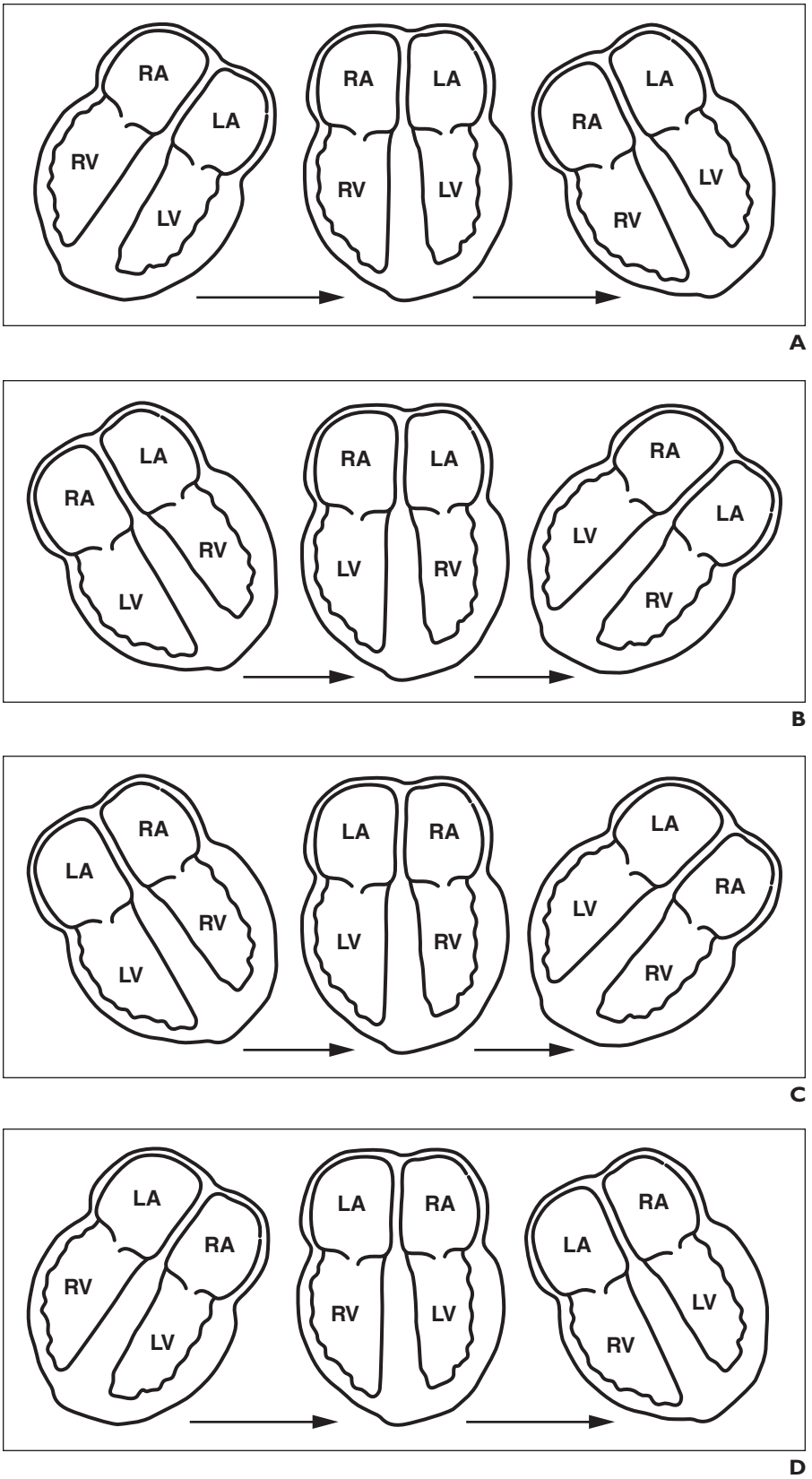

Fig. 4—Drawings show variations in looping and horizontal shift (version) of cardiac apex. RA = right atrium, LA = left atrium, RV = right ventricle, LV = left ventricle.
A, Normal configuration: situs solitus with D looping results in atrioventricular concordance. Cardiac mass normally shifts from right to left, transitioning from dextroversion to mesoversion and ultimately resulting in levoversion (levocardia).
B, Situs solitus with L looping results in atrioventricular discordance. Cardiac mass usually shifts from left to right, leading to dextroversion (dextrocardia).
C, Situs inversus with L looping results in atrioventricular concordance. Cardiac mass shifts from left to right, leading to dextroversion (dextrocardia).
D, Situs inversus with D looping results in atrioventricular discordance. Cardiac mass shifts from right to left, leading to levoversion (levocardia).

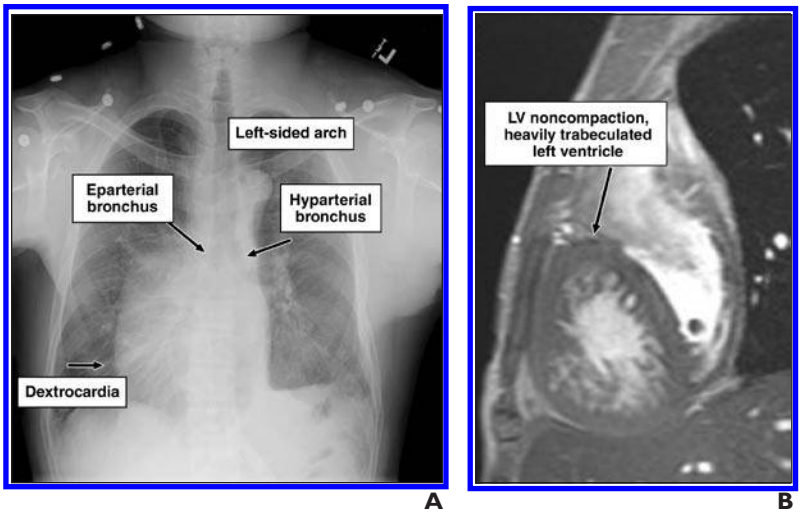

Fig. 5—46-year-old man with situs solitus, dextrocardia, and left ventricular noncompaction. Situs solitus with dextrocardia has 90% association with congenital heart disease. Most common association is right heart obstruction such as tricuspid atresia or pulmonary atresia.
A, Posteroanterior chest radiograph shows situs solitus and dextrocardia. Stomach bubble is on left.
B, Short axis bright-blood image shows heavy trabeculation of anterior left ventricle (LV) in this patient with noncompaction cardiomyopathy.

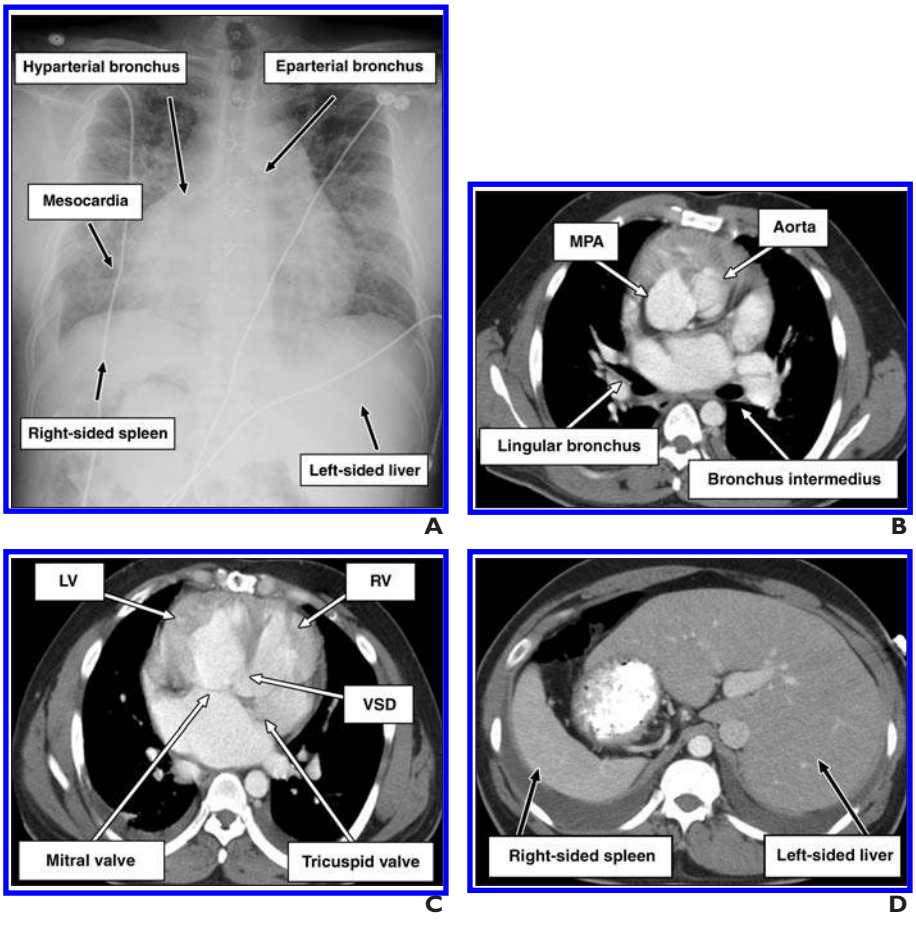

Fig. 6—33-year-old man with situs inversus and mesocardia who has transposition of great arteries and endocardial cushion defect. Risk of congenital heart disease (CHD) for situs inversus with mesocardia is similar to that of normal configuration (0.8%). When CHD is present, most common association, as in this patient, is corrected transposition of great arteries.
A, Posteroanterior chest radiograph shows situs inversus totalis with mesocardia. Note pulmonary overcirculation (shunt vascularity) and small right pleural effusion.
B and **C,** Contrast-enhanced chest CT scans show thoracic situs inversus. Aorta is anterior and to left of pulmonary artery. Note atrioventricular discordance and ventriculoarterial discordance, consistent with corrected transposition of great arteries. Mitral and tricuspid valves are located at same level, indicating endocardial cushion defect. VSD indicates ventricular septum defect; MPA, main pulmonary artery; LV, left ventricle; RV, right ventricle.
D, Contrast-enhanced abdominal CT scan shows abdominal situs inversus.

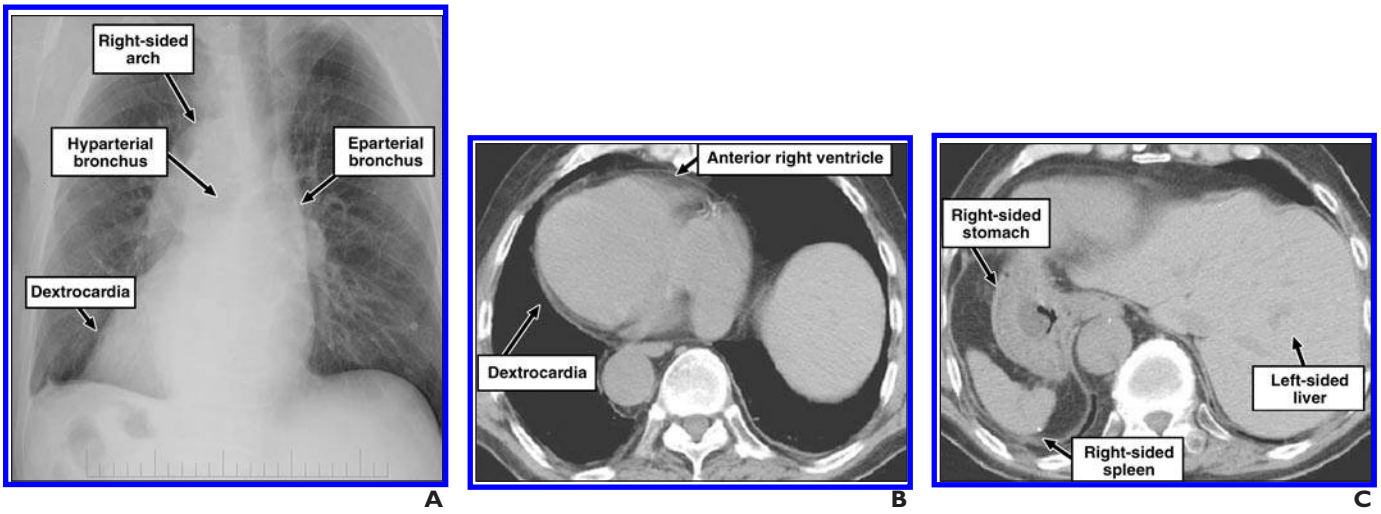

Fig. 7—74-year-old man with situs inversus totalis. Situs inversus totalis has incidence of 1 in 10,000 live births, of which 3–5% have congenital heart disease.
A, Posteroanterior chest radiograph shows mirror-image bronchial anatomy, right-sided cardiac apex, and right-sided stomach bubble, consistent with situs inversus totalis.
B, Unenhanced chest CT scan shows cardiac apex to be right-sided with anterior right ventricle.
C, Unenhanced CT of abdomen shows abdominal situs inversus with left-sided liver and right-sided stomach and spleen.

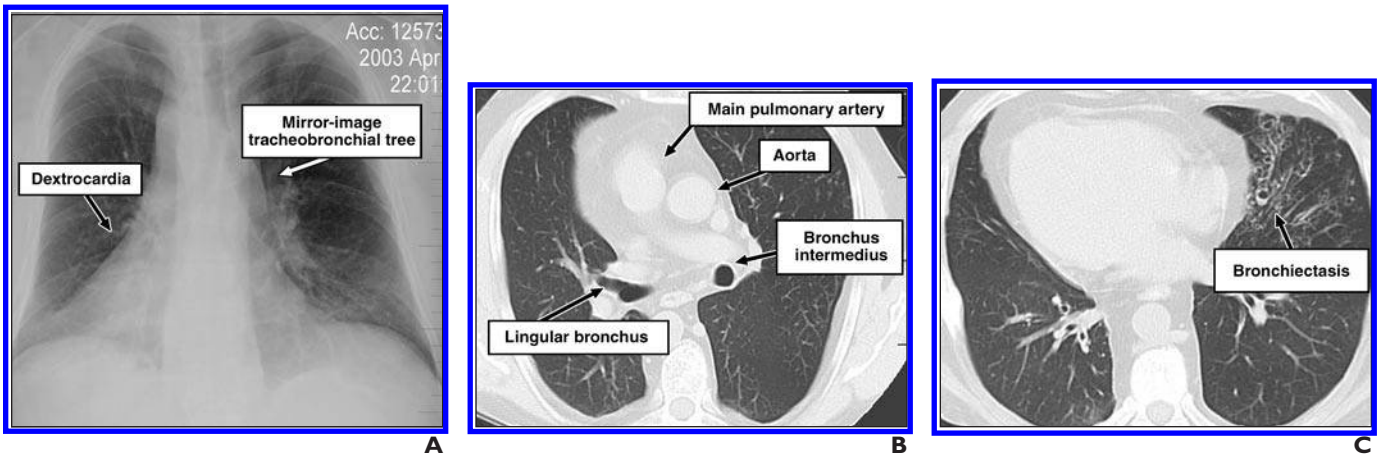

Fig. 8—47-year-old man with Kartagener's syndrome.
A, Posteroanterior chest radiograph shows thoracic situs inversus with dextrocardia. Note tram-tracking and tubular parenchymal opacities in left lung, which are consistent with bronchiectasis.
B, Lung window view from chest CT shows mirror-image bronchial anatomy, with right-sided lingular bronchus and left-sided bronchus intermedius.
C, CT image at lung window setting shows bronchiectasis in left-sided middle lobe.

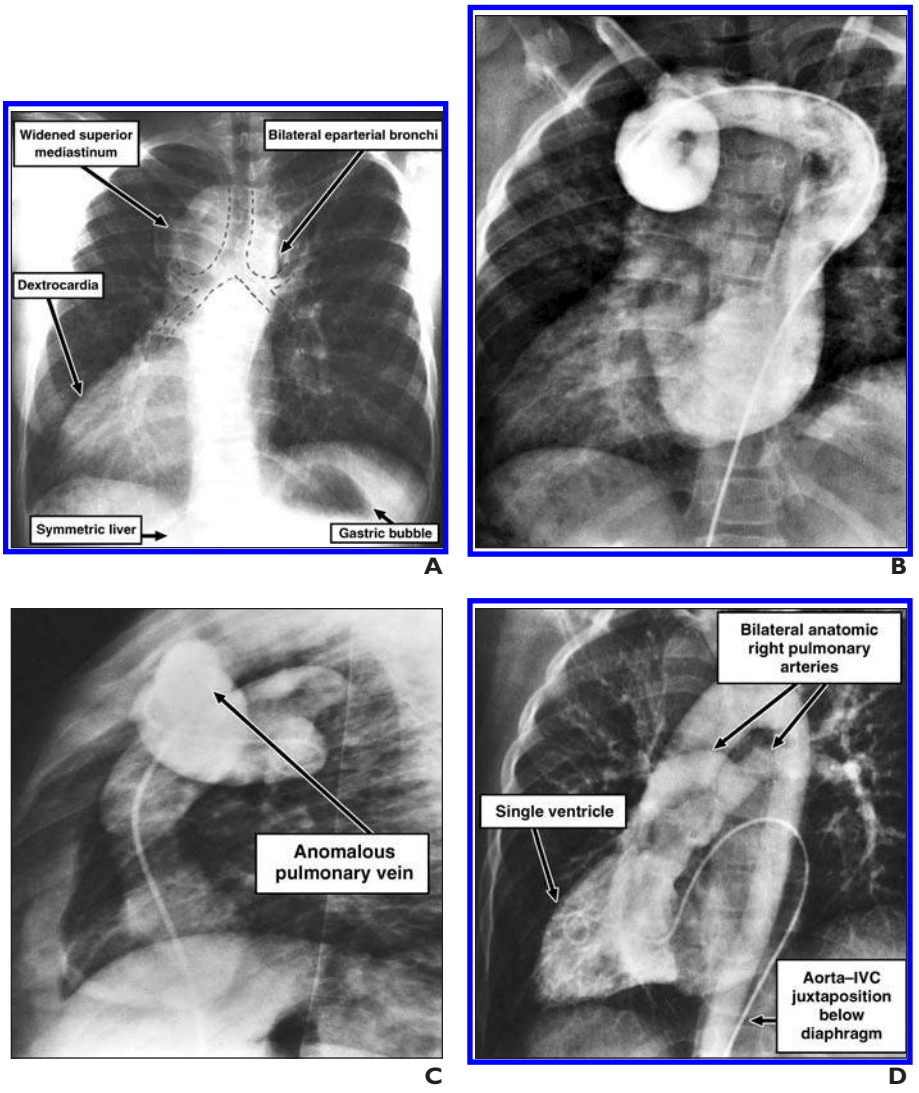

Fig. 9—Asplenia and supracardiac total anomalous pulmonary venous return. Asplenia has 99–100% association with congenital heart disease. (Reprinted with kind permission of Springer Science and Business Media [1])
A, Posteroanterior chest radiograph shows bilateral right-sided (eparterial) bronchi and dextrocardia. Liver is symmetric and stomach is left-sided.
B, Frontal view of venogram. Catheter is advanced from right-sided inferior vena cava into common atrium with its tip in anomalous pulmonary vein. Contrast material opacifies total anomalous pulmonary venous return, supracardiac type.
C, Lateral view from venogram. Anomalous pulmonary vein is anterior to trachea and may simulate mass on lateral chest radiograph.
D, Ventriculogram shows single left ventricle with D malposition of great arteries and atrioventricular canal. Pulmonary arteries show bilateral right-sided anatomy. IVC = inferior vena cava.

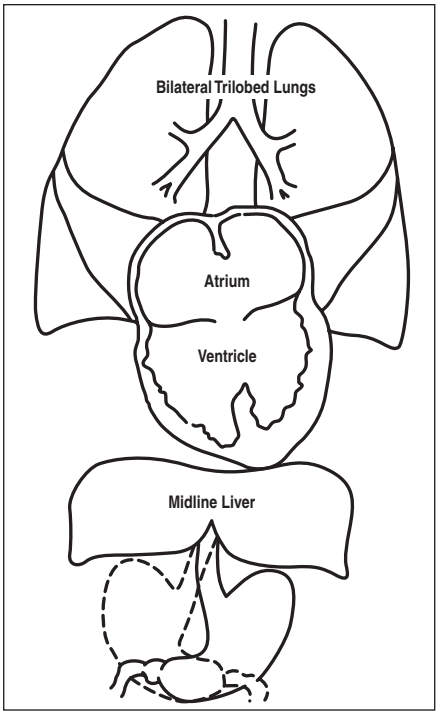

Fig. 10—Schematic diagram of asplenia. Bilateral trilobed lungs and bilateral eparterial bronchi are characteristic. Liver is often midline, spleen is absent, and position of stomach is variable. Bowel malrotation is common. Congenital heart disease is nearly universal. Associated cardiac defects are generally severe and include common atrium and single ventricle with pulmonary stenosis or atresia.

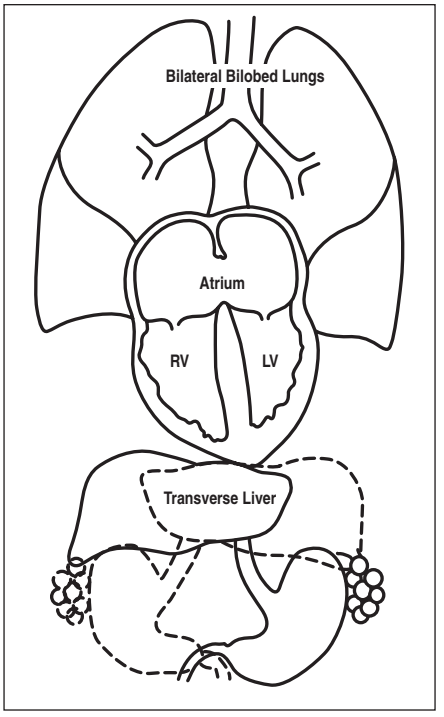

Fig. 11—Schematic diagram of polysplenia. Bilateral bilobed lungs and bilateral hyparterial bronchi are characteristic. Liver is often midline; positions of multiple small rounded spleens and stomach are variable. Bowel malrotation is common. Congenital heart disease occurs in 75% of these patients. Cardiac defects are milder than in asplenia and include endocardial cushion defects. Transposition and severe pulmonic stenosis are rare. Left-sided obstructive lesion such as coarctation of aorta may occur. RV = right ventricle, LV = left ventricle.

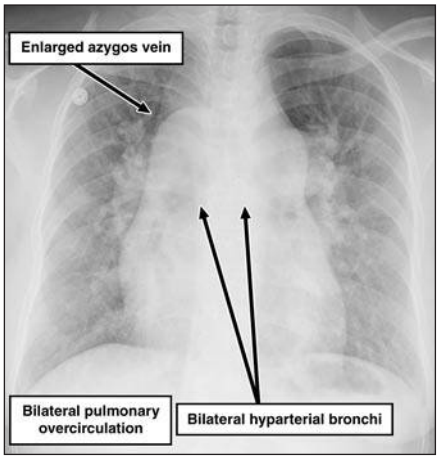

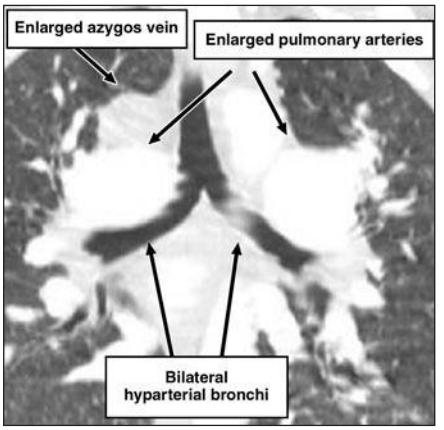

Fig. 12—30-year-old woman with polysplenia syndrome. Congenital heart disease is associated in 75% of these patients. This patient had history of repaired endocardial cushion-type atrial septal defect.
A, Posteroanterior chest radiograph shows cardiomegaly with pulmonary overcirculation (shunt vascularity). Note bilateral hyparterial bronchi and enlarged azygos vein.
B, Coronal reformatted CT image shows bilateral left-sided (hyparterial) bronchial anatomy. Pulmonary arteries lie above bronchi, and dilated azygos arch is cephalad to right pulmonary artery.

(Fig. 12 continues on next page)

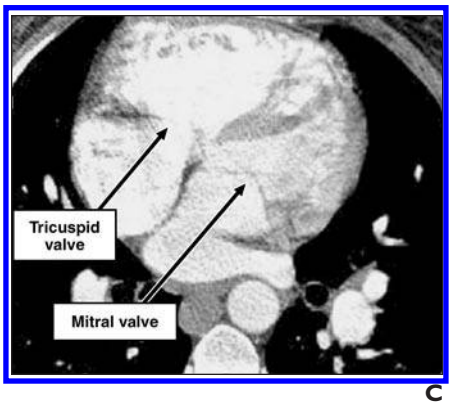

C

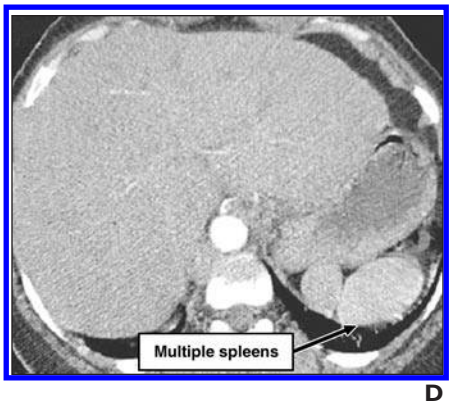

D

Fig. 12 (continued)—30-year-old woman with polysplenia syndrome. Congenital heart disease is associated in 75% of these patients. This patient had history of repaired endocardial cushion-type atrial septal defect.
C, Contrast-enhanced chest CT scan at level of heart shows that mitral and tricuspid valves are at same level, consistent with endocardial cushion defect. Right ventricle, anteriorly located, is dilated and hypertrophied. Note azygos continuation of inferior vena cava; enlarged unenhanced azygos vein is similar in caliber and just to right of descending aorta.
D, Contrast-enhanced CT scan of upper abdomen shows several small rounded spleens. Intrahepatic segment of inferior vena cava is absent.

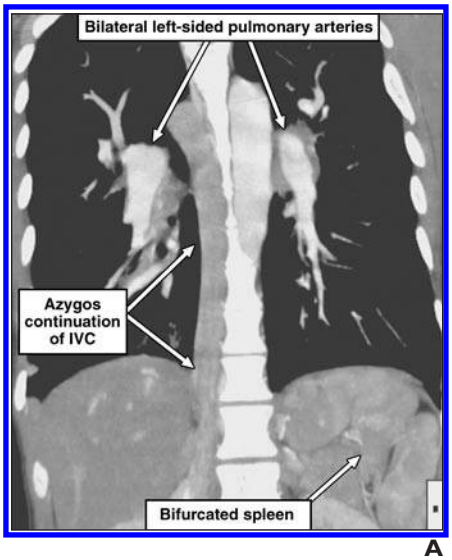

A

B

Fig. 13—23-year-old woman with F-anisosplenia, variant of heterotaxy that occurs in females characterized by bilateral left-sidedness and bifurcated spleens, nearly always associated with severe cyanotic congenital heart disease.
A, Coronal reformatted contrast-enhanced CT scan shows bilateral anatomic left pulmonary arteries and azygos continuation of inferior vena cava (IVC). Note bifurcated spleen in left upper quadrant of abdomen.
B, Axial contrast-enhanced CT scan shows single ventricle and atrioventricularis communis.
C, Oblique reformatted contrast-enhanced CT image shows bilateral Blalock-Taussig shunts, left partially calcified. Coronary sinus is absent, and no hepatic venous confluence is present. Each hepatic vein drains directly into common atrium.
D, Oblique reformatted contrast-enhanced CT image shows single ventricle giving rise to both great vessels. Aorta is anterior, superior, and to right of pulmonary artery, consistent with D malposition. Pulmonary artery is stenotic.

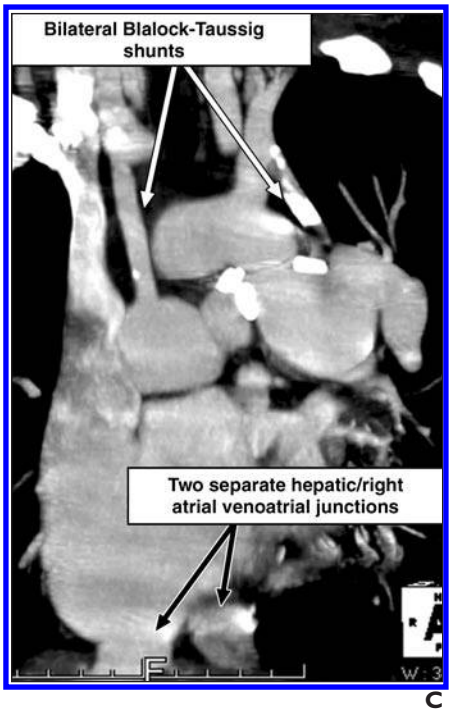

C

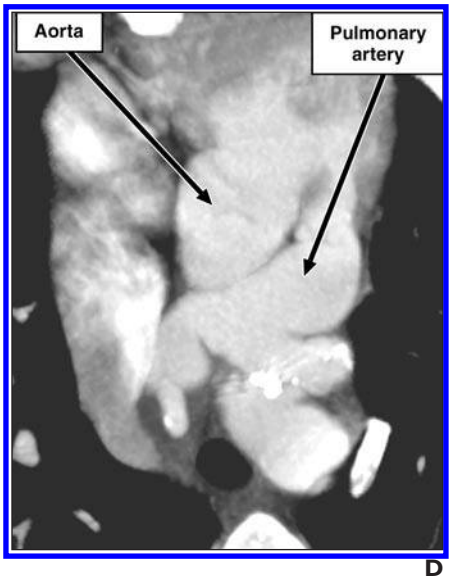

D

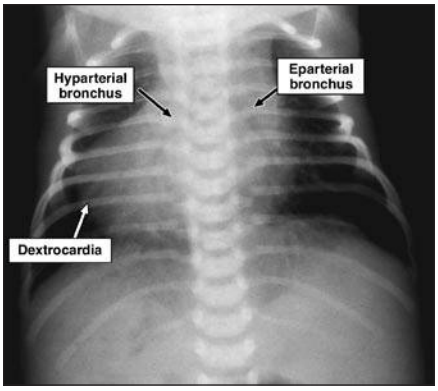

Fig. 14—5-day-old boy with dyspnea. Posteroanterior chest radiograph shows situs solitus totalis with dextrocardia, which is associated with congenital heart disease in 3–5% of patients. Note cardiomegaly and pulmonary overcirculation in this patient with single ventricle.

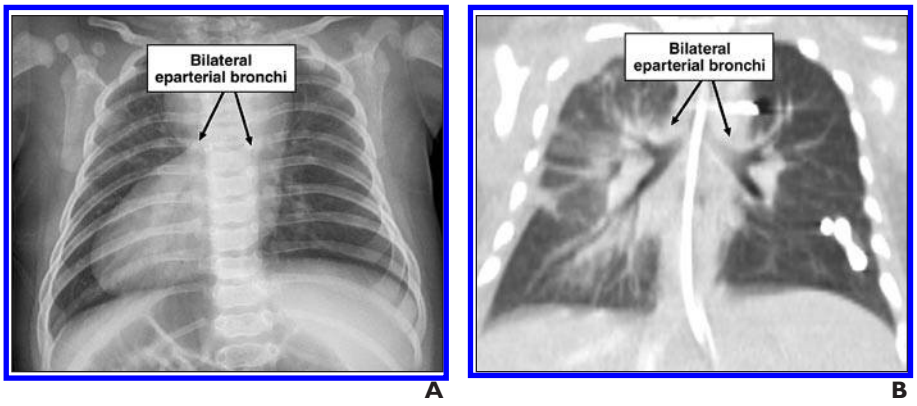

Fig. 15—5-month-old cyanotic girl with asplenia, which has 99–100% association with severe congenital heart disease. Patient was diagnosed with atrioventricular canal, double-outlet right ventricle, and pulmonary atresia.
A, Posteroanterior chest radiograph shows bilateral eparterial (right-sided) bronchi typical of asplenia.
B, Coronal reformatted CT image confirms presence of bilateral eparterial bronchi.

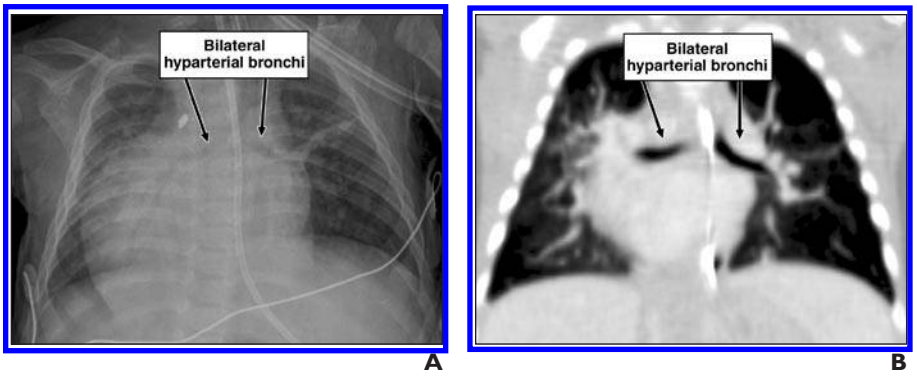

Fig. 16—6-month-old girl with polysplenia, which has 75% association with congenital heart disease. She was diagnosed with atrioventricular canal and coarctation of aorta.
A, Posteroanterior chest radiograph shows bilateral hyparterial bronchi. Note cardiomegaly, dextrocardia, and pulmonary overcirculation. Liver is symmetric.
B, Coronal reformatted CT image confirms presence of bilateral hyparterial bronchi.

FOR YOUR INFORMATION

This article is available for CME credit. See www.arrs.org for more information.

This article has been cited by:

1. Amna Al-Arnawoot, John Kavanagh, Elsie T. Nguyen. 2021. Type 2 bridging bronchus with left pulmonary artery sling. *Cardiology in the Young* **31**:10, 1701-1703. [Crossref]
2. Muhammad I. Aumeerally, Yi-Tzu Lin, Terence C. Chua. 2021. Ambiguous Anatomy and Its Pain. *Gastroenterology* **160**:4, e13-e15. [Crossref]
3. Ramiah Rajeshkannan. Sequential Segmental Approach to CHD 107-128. [Crossref]
4. Viralam S. Kiran, Sandeep Choudhary, Amira Shaik, Karthik Gadabanahalli, Vimal Raj, Venkatraman Bhat. 2020. The Spectrum of Cardiac Anomalies Associated with Heterotaxy: A Single-Center Study of a Large Series Based on Computed Tomography. *Pediatric Cardiology* **41**:7, 1414-1424. [Crossref]
5. Janaka Lovell, Jonathan Sivakumar, Shiran Wijeratne. 2020. Incidental abdominal heterotaxy syndrome. *ANZ Journal of Surgery* **90**:5, 911-912. [Crossref]
6. Fatemah Jeragh, Ismaiel Aljazzaf, Haitham Al Khayyat. 2020. Laparoscopic sleeve gastrectomy in polysplenia syndrome/left isomerism: A case report. *International Journal of Surgery Case Reports* **75**, 488-491. [Crossref]
7. Sarv Priya, Prashant Nagpal, Arun Sharma, Niraj N. Pandey, Priya Jagia. 2019. Imaging Spectrum of Double-Outlet Right Ventricle on Multislice Computed Tomography. *Journal of Thoracic Imaging* **34**:5, W89-W99. [Crossref]
8. Lucas Samuel Perinazzo Pauvels, Felipe Welter Langer, Daiane dos Santos, Carlos Jesus Pereira Haygert. 2018. Heterotaxy syndrome. *Radiologia Brasileira* **51**:5, 344-345. [Crossref]
9. Mary M. Salvatore, Ronaldo Collo Go, Monica A. Pernia M.. The Trachea and Bronchi 23-42. [Crossref]
10. E. Dees, S. Baldwin. Heart Development 380-398. [Crossref]
11. Ellen Dees, H. Scott Baldwin. Developmental Biology of the Heart 724-740.e3. [Crossref]
12. Shahab Abid, Dawar Khan. 2017. A Rare Cause of Recurrent Constipation With Abdominal Pain and Distension. *Gastroenterology* . [Crossref]
13. Toru Nakano, Takashi Kamei, Yu Onodera, Naoto Ujiie, Noriaki Ohuchi. 2017. Thoracoscopic surgery in the prone position for esophageal cancer in patients with situs inversus totalis: A report of two cases. *International Journal of Surgery Case Reports* **31**, 43-46. [Crossref]
14. E. Dees, S. Baldwin. . [Crossref]
15. . Heterotaxia Syndromes 312-315. [Crossref]
16. Masanori Matsuda, Hidetake Amemiya, Naohiro Hosomura, Masahito Ogiku, Hideki Fujii. 2015. Hepatic resection for hepatocellular carcinoma in a patient with situs ambiguous with polysplenia: report of a case. *Surgery Today* **45**:6, 765-771. [Crossref]
17. Ricardo Duarte, Humberto Morais. 2015. Aortic pseudocoarctation associated with polysplenia/heterotaxy syndrome. *Revista Portuguesa de Cardiologia* **34**:1, 73.e1-73.e3. [Crossref]
18. Ricardo Duarte, Humberto Morais. 2015. Aortic pseudocoarctation associated with polysplenia/heterotaxy syndrome. *Revista Portuguesa de Cardiologia (English Edition)* **34**:1, 73.e1-73.e3. [Crossref]
19. Marinos Kontzialis, Hugo Spindola-Franco, Linda B. Haramati. Visceroatrial Situs in Congenital Heart Disease 285-303. [Crossref]
20. Christopher D. Wolla, Anthony M. Hlavacek, U. Joseph Schoepf, Andreas M. Bucher, Shahryar Chowdhury. 2013. Cardiovascular manifestations of heterotaxy and related situs abnormalities assessed with CT angiography. *Journal of Cardiovascular Computed Tomography* **7**:6, 408-416. [Crossref]
21. Daniel Bell, M Venkatesh. Asplenia syndrome . [Crossref]
22. F. Ghadouani, G. Kharrasse, T. El Harroudi, A. Sbai, K. Talby. 2013. Syndrome de polysplénie avec association exceptionnelle polysplénie–diastématomyélie. *Feuillets de Radiologie* . [Crossref]
23. Ahmed M. Tawfik, Nihal M. Batouty, Mona M. Zaky, Mohamed A. Eladalany, Ali H. Elmokadem. 2013. Polysplenia syndrome: a review of the relationship with viscero-atrial situs and the spectrum of extra-cardiac anomalies. *Surgical and Radiologic Anatomy* . [Crossref]
24. Wojciech Mazur, Marilyn J. Siegel, Tomasz Miszalski-Jamka, Robert Pelberg. Heterotaxy Syndrome 253-259. [Crossref]

25. Horacio Murillo, Michael J. Cutalo, Robert P. Jones, Michael J. Lane, Dominik Fleischmann, Carlos S. Restrepo. 2012. Pulmonary Circulation Imaging: Embryology and Normal Anatomy. *Seminars in Ultrasound, CT and MRI* **33**:6, 473-484. [Crossref]
26. W. El Guindi, M. Dreyfus, G. Carles, V. Lambert, M. Herlicoviez, G. Benoit. 2012. L'apport de l'échographie 3D dans les syndromes d'hétérotaxie : à propos de quatre cas et revue de la littérature. *Journal de Gynécologie Obstétrique et Biologie de la Reproduction* **41**:5, 489-496. [Crossref]
27. H. Scott Baldwin, Ellen Dees. Embryology and Physiology of the Cardiovascular System 699-713. [Crossref]
28. Hyun Woo Goo. 2011. Cardiac MDCT in Children: CT Technology Overview and Interpretation. *Radiologic Clinics of North America* **49**:5, 997-1010. [Crossref]
29. Lee-Anne Slater. Heterotaxy syndrome . [Crossref]
30. Calum Worsley, Yuranga Weerakkody. Heterotaxy syndrome . [Crossref]